

# FLAMINGOS Spectroscopy of New Low-Mass Members of the Young Cluster IC 348

K. L. Luhman<sup>1</sup>, Elizabeth A. Lada<sup>2,3</sup>, August A. Muench<sup>1,3</sup>, and Richard J. Elston<sup>2,3</sup>

## ABSTRACT

We present spectroscopy of candidate stellar and substellar members of the young cluster IC 348. Using the Florida Multi-Object Imaging Near-Infrared Grism Observational Spectrometer with the 4 meter telescope at Kitt Peak National Observatory, we have obtained multi-object moderate-resolution ( $R = 1000$ )  $J$ - and  $H$ -band spectra of 66 infrared sources ( $H = 12$ - $17$ ) toward IC 348, many of which are difficult to observe spectroscopically at optical wavelengths ( $I > 20$ ) because they are highly reddened and/or intrinsically cool and red. We have also observed 19 known cluster members that have optical spectral types available from previous work. By using these latter sources as the spectral classification standards, we have identified 14 new members of the cluster with types of M2-M6 in the sample of 66 new objects. Two additional objects exhibit types of  $>M8.5$ , but cannot be conclusively classified as either field dwarfs or cluster members with available data. We have estimated extinctions, luminosities, and effective temperatures for these 16 M-type objects, placed them on the H-R diagram, and used the evolutionary models of Chabrier & Baraffe to estimate their masses. If the two candidates at  $>M8.5$  are indeed members, they should be among the least massive known brown dwarfs in IC 348 ( $M/M_{\odot} \sim 0.01$ ).

*Subject headings:* infrared: stars — stars: evolution — stars: formation — stars: low-mass, brown dwarfs — stars: pre-main sequence

## 1. Introduction

Young stellar clusters embedded within molecular clouds are valuable laboratories for studying the birth of stars, brown dwarfs, and planets (Lada & Lada 2003). Because of its rich and compact nature ( $\sim 400$  members,  $D \sim 20'$ ) and its proximity to the Sun ( $d = 315$  pc), the IC 348 cluster in the Perseus molecular cloud is a particularly appealing population. Over the last decade, the identification and characterization of the contents of young clusters like IC 348 have benefited from advancements in detectors, instruments, and telescopes. The area and sensitivity of near-infrared (IR) imaging surveys of IC 348 have progressively increased (Lada & Lada 1995; Luhman et al. 1998; Muench et al. 2003; Preibisch et al. 2003), resulting in improved constraints on the mass distribution of cluster members derived from statistical analysis of luminosity functions. A similar trend in optical CCD imaging of IC 348 has extended the identification of individual candidate members to lower masses, higher reddenings, and larger distances from the cluster center (Herbig 1998; Luhman 1999; Luhman et al. 2003). To assess membership and measure spectral types for

---

<sup>1</sup>Harvard-Smithsonian Center for Astrophysics, 60 Garden St., Cambridge, MA 02138, USA; kluhman@cfa.harvard.edu.

<sup>2</sup>Department of Astronomy, The University of Florida, Gainesville, FL 32611, USA.

<sup>3</sup> Visiting Astronomer, Kitt Peak National Observatory, National Optical Astronomy Observatory, which is operated by the Association of Universities for Research in Astronomy, Inc., under cooperative agreement with the National Science Foundation.

these candidates, increasingly sophisticated spectrometers have been employed, consisting of optical (Herbig 1998) and near-IR (Luhman et al. 1998) single-slit instruments and optical multi-slit devices (Luhman 1999; Luhman et al. 2003).

Because of their small angular sizes and the fact that their obscured members are brightest beyond  $1 \mu\text{m}$ , embedded clusters are well-suited for multi-object spectroscopy at near-IR wavelengths. One of the first instruments of this kind is the Florida Multi-Object Imaging Near-IR Grism Observational Spectrometer (FLAMINGOS, Elston (1998)), which we have recently used to expand our spectroscopic work in IC 348, particularly among the members at low masses and high reddenings that are difficult to reach with optical spectroscopy. In this paper, we describe the selection of our spectroscopic targets and the FLAMINGOS observations (§ 2), measure the spectral types of the targets (§ 3.1), assess their membership in IC 348 (§ 3.2), estimate the extinctions, effective temperatures, and bolometric luminosities for 14 confirmed members and 2 late-type candidate members and interpret their positions on the Hertzsprung-Russell (H-R) diagram with theoretical evolutionary models (§ 3.3), and discuss the implications of this work (§ 4).

## 2. Observations

For the FLAMINGOS spectroscopy in this study, we selected candidate members of IC 348 appearing in the optical and IR color-magnitude diagrams from Luhman et al. (2003). We also included known cluster members that have optical spectral types from Luhman (1999) and Luhman et al. (2003), which will be used as the standards during the classification of the candidates in § 3.1. After designing a slit mask for a set of these objects, we included additional slitlets as space allowed for faint IR sources from the images of Muench et al. (2003). In this way, useful spectra were obtained for 19 known members and 66 previously unclassified sources.

The spectrograph was operated with the 4 m telescope at Kitt Peak National Observatory on the nights of 2003 January 15-17 and December 10 and 13. Spectra were obtained through a different slit mask on each of the five nights. For each mask, the number of exposures, integration time per exposure, and targets are listed in Table 1. The instrument employed a  $2048 \times 2048$  HgCdTe HAWAII-2 array, which yielded a plate scale of  $0''.316 \text{ pixel}^{-1}$  and a field of view of a  $10''.8 \times 10''.8$  on the 4 m telescope. The width of each mask slitlet was  $0''.95$  (3 pixels). This configuration produced full coverage from 1.1 to  $1.8 \mu\text{m}$  with a spectral resolution of  $R = \lambda/\Delta\lambda \sim 1000$ . The targets were dithered between two positions separated by  $4''$  along the slitlets. A nearby G dwarf was also observed through a long slit for the correction of telluric absorption. After dark subtraction and flat-fielding, adjacent images along the slit were subtracted from each other to remove sky emission. The sky-subtracted images were aligned and combined. A spectrum of each target was then extracted, wavelength calibrated with OH airglow lines, and divided by the spectrum of the telluric standard. The intrinsic spectral slope and absorption features of the standard were removed by multiplying by the solar spectrum.

## 3. Analysis

### 3.1. Spectral Types

To measure spectral types for the candidate members of IC 348 that we have observed spectroscopically, we begin by examining the spectra of the known members with optical classifications in our sample. These

members consist of sources 12A (A3), 6 (G3), 59 (K2), 120 (M2.25), 122 (M2.25), 207 (M3.5), 210 (M3.5), 76 (M3.75), 95 (M4), 266 (M4.75), 112 (M4.75), 230 (M5.25), 555 (M5.75), 298 (M6), 329 (M7.5), 405 (M8), 611 (M8), 613 (M8.25), and 603 (M8.5), where the identifications and spectral types are from Luhman (1999) and Luhman et al. (2003). The spectra for the known members are shown in order of optical type in Figures 1 and 2 and are labeled with only their optical classifications. Because the telluric correction was not always accurate between 1.345 and 1.495  $\mu\text{m}$ , data in this wavelength range is omitted. The strongest atomic and molecular features in these spectra are labeled, which consist of the H I and Mg I lines and the steam bands. Other weaker lines are detected as well, identifications for which can be found in Wallace et al. (2000), Meyer et al. (1998), and McGovern et al. (2004). As demonstrated in Figures 1 and 2, the detected IR spectral features change monotonically with optical type and thus can be used to classify the new candidates observed in this work. The steam bands are particularly useful for measuring spectral types of late-type objects (Willing et al. 1999; Reid et al. 2001; Leggett et al. 2001; Luhman, Peterson, & Megeath 2004), as shown by the rapid change in the decrement at 1.35  $\mu\text{m}$  and in the broad absorption at both ends of the *H*-band. Because of the broad nature of these bands, they can be measured at low spectral resolution. Meanwhile, the narrow atomic lines become weak and difficult to detect at late M types, and thus higher resolution becomes unnecessary. Therefore, the signal-to-noise of the coolest and faintest objects can be improved by smoothing to a lower resolution without compromising the spectral diagnostics. The spectra for objects later than M6 are smoothed to a resolution of  $R = 200$  in Figure 2, while the earlier objects in Figures 1 are shown at a resolution of  $R = 500$ .

Because near-IR steam absorption bands are stronger in young objects than in field dwarfs at a given optical spectral type (Luhman & Rieke 1999; Lucas et al. 2001; McGovern et al. 2004), spectral types of young objects derived from steam with dwarf standards will be systematically too late. Instead, to arrive at accurate spectral types, optically-classified young objects rather than dwarfs should be used when measuring spectral types of young sources from steam (Luhman & Rieke 1999; Luhman et al. 2003), which is the approach we adopt in the following classification of the candidate members of IC 348.

Extinction within the natal cloud of IC 348 results in large variations in the slopes of the observed spectra in our sample. To facilitate the comparison of the steam band depths between the candidates and the optically-classified known members, we have dereddened all spectra with detectable steam to the same slope as measured by the ratios of fluxes at 1.32 and 1.68  $\mu\text{m}$ . These dereddened spectra are not meant to be precise estimates of the intrinsic, unreddened appearance of these stars since the slopes likely vary with spectral type. After dereddening, for each candidate we measured a spectral type by visually comparing the steam bands and atomic lines in its spectrum to those in the data of the optically-classified members. Through this analysis, we find that 16 of the 66 new objects in our sample exhibit M types. Within the sequence of optically-classified members in Figures 1 and 2, these 16 sources have been inserted and are labeled with their identifications and the types derived from these IR spectra. These objects are also listed Table 2. The other 50 sources lack steam absorption and therefore are earlier than  $\sim\text{M0}$ . More accurate classifications for these early-type stars are not possible in most cases because the signal-to-noise is too low to measure the atomic lines. However, the spectral type constraints are sufficient to indicate that all of these 50 objects without steam are probably field stars (§ 3.2). These stars are listed in Table 3.

A few of the new M-type objects require additional comments. Continuum emission from cool circumstellar material should be much weaker than photospheric emission in bands as short as *J* and *H*, particularly given that a small fraction of members of IC 348 have noticeable excess emission at *K* (Haisch, Lada, & Lada 2001). However, for two of the new sources, 202 and 272, the *H*-band atomic lines are weaker than expected for the spectral type implied by the steam bands, which is suggestive of modest continuum veiling. The

presence of veiling is not surprising given the strong H emission in both stars, which is a signature of active accretion, and the large  $K$ -band excess in source 202. Because of this possible veiling, the uncertainties in the derived spectral types for these stars are larger than for the other new M-type objects. Finally, the steam absorption bands in sources 1050 and 2103 are stronger than in the latest optically-classified member in our spectroscopic sample (M8.5). Therefore, we can place only upper limits on the spectral types of these two objects.

### 3.2. Membership

A star projected against IC 348 could be a member of the cluster or a field star in the foreground or the background. For each of the 66 previously unclassified sources in our spectroscopic sample, we employ the diagnostics described by Luhman et al. (2003) to distinguish between these possibilities.

Objects that appear near or below the main sequence when placed on the H-R diagram at the distance of IC 348 are likely to be background field stars. In the previous section, 50 stars were found to lack steam absorption, which implied spectral types earlier than M0. Some of these stars have even earlier limits based on the presence of hydrogen absorption lines. These spectral type constraints indicate that all of these stars are likely to be background field stars because of their low positions on the H-R diagram. In other words, given their faint magnitudes, these sources should be much cooler than observed if they were members of IC 348. As noted in previous studies of IC 348 and other young clusters (e.g., Luhman et al. (2003)), young stars that are seen in scattered light can appear low on the H-R diagram, even below the main sequence. Indeed, a few of the previously known members of IC 348 are subluminoous in this manner. As a result, it is possible that some of the objects that we classify as background stars in Table 3 could be scattered-light members of IC 348. Imaging of IC 348 with the *Spitzer Space Telescope* should easily identify any young objects of this kind through detections of their mid-IR excesses.

We now evaluate the membership of the remaining objects, which are the 16 M-type sources. Because IC 348 is a star-forming cluster, signatures of youth comprise evidence of membership. Examples include emission in the Brackett and Paschen series of hydrogen and excess emission at  $K$ , which are found in three of our sources. Next, the presence of significant reddening in the spectrum or colors ( $A_V > 1$ ) of a star and a position above the main sequence for the distance of IC 348 indicate that it cannot be a dwarf in the foreground or the background of the cluster, respectively. Fourteen of the new M-type objects are not field dwarfs when this criterion is applied with the extinctions estimated in the next section. The remaining two M-type sources, the ones classified as  $>M8.5$ , also appear to exhibit reddening in their spectra and colors. However, the reddenings implied by the spectra are uncertain because of the low signal-to-noise of those data while the reddenings measured from near-IR colors are uncertain because the spectral type, and thus the adopted intrinsic colors, are not well constrained. Therefore, with this diagnostic, we cannot rule out the possibility that these two sources are foreground dwarfs.

Pre-main-sequence objects can also be distinguished from field dwarfs and giants with spectral features that are sensitive to surface gravity, a variety of which have been identified for cool objects at both optical (Martín et al. 1996; Luhman 1999; McGovern et al. 2004) and near-IR (Luhman et al. 1998; Gorlova et al. 2003; McGovern et al. 2004) wavelengths. For instance, the broad plateaus observed in the  $H$  and  $K$  spectra of late-M and L dwarfs (Reid et al. 2001; Leggett et al. 2001) are absent in data for young objects, resulting in sharply peaked, triangular continua (Lucas et al. 2001), as illustrated by the known late-type members of IC 348 in Figure 2. The  $H$ -band spectra of the new M-type sources appear to exhibit this signature of

youth, but we do not consider this definitive evidence of membership since we do not have spectra of field dwarfs and giants to compare to these sources.

The results of our analysis of the membership of the 16 new M-type sources are compiled in Table 2. In summary, we have found evidence of membership in IC 348 for 14 of the 16 new M-type sources. The remaining two objects are promising candidate members that require additional data to determine their membership definitively. The masses and reddenings of these 16 sources relative to those of the previously known members of IC 348 are illustrated by the diagram of  $J - H$  versus  $H$  in Figure 3.

### 3.3. H-R Diagram

In this section, we estimate effective temperatures and bolometric luminosities for the 14 new members of IC 348, place these data on the H-R diagram, and use theoretical evolutionary models to infer masses and ages. We also estimate the values of these properties expected for the two late-M candidate members, 1050 and 2103, if they are bonafide members.

For each source, we adopt the average extinction measured from its  $I - Z$  and  $J - H$  colors. The extinction from  $I - Z$  is computed in the manner described by Luhman et al. (2003). For  $J - H$ , we compute extinction from the color excess relative to dwarf colors at the spectral type in question, with the exception of sources 202 and 1124. Because these stars exhibit large  $K$ -band excesses, their  $J - H$  and  $H - K_s$  colors are instead dereddened to the locus observed for classical T Tauri stars (Meyer et al. 1997). Spectral types are converted to temperatures with the temperature scale from Luhman et al. (2003). Bolometric luminosities are estimated by combining  $J$ -band measurements, a distance modulus of 7.5, and bolometric corrections described by Luhman (1999). The estimates of extinctions, temperatures, and luminosities for the 16 M-type sources are listed in Table 2.

These temperatures and luminosities can be interpreted in terms of masses and ages with theoretical evolutionary models. We select the models of Baraffe et al. (1998) and Chabrier et al. (2000) because they provide the best agreement with observational constraints (Luhman et al. 2003). The 14 new members of IC 348 and the two candidate members are plotted with these models on the H-R diagram in Figure 4. For comparison, we also include the sequence of previously known members from Luhman et al. (2003), which encompasses the positions of the new sources. The 14 new members at M2-M6 exhibit masses of 0.45 to 0.08  $M_\odot$  according to the adopted models. Meanwhile, if the two late-type candidates are cluster members, then they should have masses less than 0.04  $M_\odot$ . Adopting the median cluster age of  $\sim 2$  Myr implies masses of only  $\sim 0.01 M_\odot$  for these two sources.

## 4. Discussion

We have demonstrated that multi-object spectroscopy at near-IR wavelengths can be successfully used to efficiently obtain accurate spectral classifications ( $\pm 0.5$ -1 subclass at M types) for large numbers of faint candidate young stars and brown dwarfs in embedded clusters. Our FLAMINGOS spectroscopy of 66 IR sources toward IC 348 has resulted in the discovery of 14 new members, several of which are highly reddened and inaccessible at optical wavelengths. These sources exhibit spectral types of M2-M6, corresponding to masses from 0.45  $M_\odot$  to near the hydrogen burning mass limit. Two additional sources in our spectroscopic sample exhibit strong steam absorption bands that are indicative of types later than M8.5. If these objects

are members of IC 348 rather than field dwarfs, they should have masses of  $\sim 0.01 M_{\odot}$ , and thus comprise the least massive known brown dwarfs in the cluster. Accurate spectral types for these two candidates will require either optical spectroscopy or IR spectra at higher signal-to-noise than provided in this work. Classification of the latter data would require IR spectra of optically-classified young objects at types later than the limit of M8.5 in our sample. Near-IR spectra at higher signal-to-noise also would provide the measurements of gravity-sensitive features and reddening that are needed to conclusively establish these candidates as either field dwarfs or young members of IC 348.

K. L. was supported by grant NAG5-11627 from the NASA Long-Term Space Astrophysics program. We thank Nick Raines for invaluable technical support and thank Bruno Ferreira, Charles Lada, Joanna Levine, Nick Raines, Noah Rashkind, Carlos Roman, Aaron Steinhauer and Andrea Stolte for mask preparation and assistance with the observations. The FLAMINGOS data were obtained under the NOAO Survey Program “Towards a Complete Near-Infrared Imaging and Spectroscopic Survey of Giant Molecular Clouds” (PI: E. Lada) and supported by NSF grants AST97-3367 and AST02-02976 to the University of Florida. FLAMINGOS was designed and constructed by the IR instrumentation group (PI: R. Elston) at the Department of Astronomy at the University of Florida with support from NSF grant AST97-31180 and Kitt Peak National Observatory.

## REFERENCES

- Baraffe, I., Chabrier, G., Allard, F., & Hauschildt, P. H. 1998, *A&A*, 337, 403
- Chabrier, G., Baraffe, I. Allard, F., & Hauschildt, P. H. 2000, *ApJ*, 542, 464
- Elston, R. 1998, *Proc. SPIE*, 3354, 404
- Gorlova, N. I., Meyer, M. R., Rieke, G. H., & Liebert, J. 2003, *ApJ*, 593, 1074
- Haisch, K. E., Lada, E. A., & Lada, C. J. 2001, *AJ*, 121, 2065
- Herbig, G. H. 1998, *ApJ*, 497, 736
- Lada, C. J., & Lada, E. A. 2003, *ARA&A*, 41, 57
- Lada, E. A., & Lada, C. J. 1995, *AJ*, 109, 1682
- Leggett, S. K., Allard, F., Geballe, T. R., Hauschildt, P. H., & Schweitzer, A. 2001, *ApJ*, 548, 908
- Lucas, P. W., Roche, P. F., Allard, F., & Hauschildt, P. H. 2001, *MNRAS*, 326, 695
- Luhman, K. L. 1999, *ApJ*, 525, 466
- Luhman, K. L., Peterson, D. E., & Megeath, S. T. 2004, *ApJ*, in press
- Luhman, K. L., & Rieke, G. H. 1999, *ApJ*, 525, 440
- Luhman, K. L., Rieke, G. H., Lada, C. J., & Lada, E. A. 1998, *ApJ*, 508, 347
- Luhman, K. L., Stauffer, J. R., Muench, A. A., Rieke, G. H., Lada, E. A., Bouvier, J., & Lada, C. J. 2003, *ApJ*, 593, 1093

- Martín, E. L., Rebolo, R., & Zapatero Osorio, M. R. 1996, *ApJ*, 469, 706
- McGovern, M. R., Kirkpatrick, J. D., McLean, I. S., Burgasser, A. J., Prato, L., & Lowrance, P. J. 2004, *ApJ*, 600, 1020
- Meyer, M. R., Calvet, N., & Hillenbrand, L. A. 1997, *AJ*, 114, 288
- Meyer, M. R., Edwards, S., Hinkle, K. H., & Strom, S. E. 1998, *ApJ*, 508, 397
- Muench, A. A., et al. 2003, *AJ*, 125, 2029
- Preibisch, T., Stanke, T., & Zinnecker, H. 2003, *A&A*, 409, 147
- Reid, I. N., Burgasser, A. J., Cruz, K. L., Kirkpatrick, J. D., & Gizis, J. E. 2001, *AJ*, 121, 1710
- Wallace, L., Meyer, M. R., Hinkle, K., & Edwards, S. 2000, *ApJ*, 535, 325
- Wilking, B. A., Greene, T. P., & Meyer, M. R. 1998, *AJ*, 117, 469

Table 1. Observing Log

Mask	Date	$N_{exp}$	$\tau_{exp}$ (min)	ID
1	2003 Jan 15	12	10	12A,59,95,112,120,202,297,333,362,410,469,574,581,584,588,594,901,917,943,951,959,998,1477,1735,2103
2	2003 Jan 16	12	10	6,207,210,230,266,298,405,485,546,555,745,4053
3	2003 Jan 17	4	10	222,329,392,603,611,613
4	2003 Dec 10	12	5	109,112,122,267,356,411,444,466,502,509,1007,1020,1021,1050,1062,1555,1729,1742,3076,3104,3117,3215
5	2003 Dec 13	8	5	76,181,233,238,258,272,274,375,377,402,429,448,1110,1124,1139,1142,1167,1172,1173,1194,22253



Table 2. New Members and Candidate Members of IC 348

ID	$\alpha(\text{J2000})^{\text{a}}$ h m s	$\delta(\text{J2000})^{\text{a}}$ ° ' "	Spectral Type	Adopt	Member <sup>b</sup> -ship	$T_{\text{eff}}^{\text{c}}$	$A_J$	$L_{\text{bol}}$	$R - I^{\text{d}}$	$I^{\text{e}}$	$I - Z^{\text{f}}$	$J - H^{\text{g}}$	$H - K_s^{\text{g}}$	$K_s^{\text{g}}$
181	03 44 35.89	32 15 53.4	M2-M3	M2.5	$A_V$	3488	0.60	0.15	...	14.90	0.64	0.88	0.24	11.96
202	03 44 34.28	32 12 40.7	M2.5-M4.5	M3.5	$A_V$ ,e,ex	3342	2.88	0.12	...	20.17	1.33	2.00	1.35	12.16
233	03 44 41.88	32 17 56.7	M4-M5	M4.5	$A_V$	3198	0.71	0.088	...	15.90	0.80	0.89	0.35	12.39
258	03 44 43.30	32 17 57.1	M3.5-M4.5	M4	$A_V$	3270	1.47	0.11	2.39	17.07	0.99	1.15	0.49	12.53
267	03 44 31.83	32 15 46.5	M4.5-M5.5	M5	$A_V$	3125	1.53	0.092	2.36	17.47	1.11	1.18	0.50	12.71
272	03 44 34.13	32 16 35.7	M3.5-M5	M4.25	$A_V$ ,e	3234	1.02	0.082	...	16.76	0.88	0.99	0.59	12.47
274	03 44 48.84	32 18 46.6	M5-M6	M5.5	$A_V$	3058	0.86	0.069	2.38	16.88	0.99	0.93	0.47	12.67
297	03 44 33.21	32 12 57.5	M4-M5	M4.5	$A_V$	3198	2.42	0.095	3.05	19.71	...	1.52	0.81	12.93
362	03 44 42.30	32 12 28.2	M4.5-M5.5	M5	$A_V$	3125	3.19	0.080	...	21.09	1.59	1.81	1.01	13.38
402	03 44 45.56	32 18 20.0	M5-M6	M5.5	$A_V$	3058	1.09	0.030	2.49	18.37	1.16	0.88	0.55	13.77
410	03 44 37.56	32 11 55.9	M3.5-M4.5	M4	$A_V$	3270	3.46	0.057	...	21.75	1.44	2.07	1.01	13.81
1050	03 44 34.90	32 15 00.0	>M8.5	...	...	<2555	$\sim 0.4$	$\sim 0.002$	...	20.34	1.21	1.00	0.60	15.58
1124	03 44 56.74	32 17 03.8	M4.5-M5.5	M5	$A_V$ ,ex	3125	2.43	0.013	2.82	20.31	1.26	1.92	1.36	14.10
1172	03 44 58.36	32 18 11.8	M5-M7	M6	$A_V$	2990	0.84	0.0061	...	19.83	1.08	0.90	0.64	15.21
1477	03 44 36.25	32 13 04.6	M5-M7	M6	$A_V$	2990	2.30	0.015	...	21.46	1.53	1.42	0.80	15.00
2103	03 44 14.92	32 13 43.5	>M8.5	...	...	<2555	$\sim 0.5$	$\sim 0.001$	...	21.94	1.21	1.08	0.78	16.40

<sup>a</sup>From the 2MASS Point Source Catalog for 297 and from Luhman et al. (2003) for the remaining objects.

<sup>b</sup>Membership in IC 348 is indicated by  $A_V \gtrsim 1$  and a position above the main sequence for the distance of IC 348 (“ $A_V$ ”),  $K$ -band excess emission (“ex”), or emission in the Brackett and Paschen lines of hydrogen (“e”). Sources 1050 and 2103 lack definitive evidence of membership from available data.

<sup>c</sup>Temperature scale from Luhman et al. (2003).

<sup>d</sup>Luhman (1999).

<sup>e</sup>From Luhman (1999) for 297 and from Luhman et al. (2003) for the remaining objects.

<sup>f</sup>Luhman et al. (2003).

<sup>g</sup>Muench et al. (2003).

Table 3. Probable Background Stars

ID	$\alpha(\text{J2000})^{\text{a}}$ h m s	$\delta(\text{J2000})^{\text{a}}$ ° ' "	$R - I^{\text{b}}$	$I^{\text{c}}$	$I - Z^{\text{d}}$	$J - H^{\text{e}}$	$H - K_s^{\text{e}}$	$K_s^{\text{e}}$
109	03 44 40.14	32 14 28.1	...	14.92	0.79	0.93	0.40	11.27
222	03 44 49.61	32 09 12.2	1.09	15.09	0.57	0.76	0.24	12.31
238	03 45 04.66	32 16 39.0	...	15.40	0.64	0.82	0.25	12.45
333	03 44 27.68	32 13 55.3	1.59	17.38	0.76	1.20	0.35	13.48
356	03 45 00.12	32 13 24.8	1.29	16.58	0.63	0.97	0.24	13.40
375	03 44 50.66	32 17 19.2	2.30	18.41	0.92	1.24	0.45	13.91
377	03 44 38.12	32 16 45.2	1.51	17.67	0.70	0.92	0.31	13.87
392	03 44 53.62	32 08 58.9	1.13	16.80	0.57	0.77	0.23	13.99
411	03 45 05.66	32 14 17.1	1.27	17.11	...	0.90	0.19	14.18
429	03 44 51.90	32 16 35.5	1.68	17.86	0.81	1.05	0.35	13.99
444	03 44 42.35	32 15 13.2	1.92	19.15	0.91	1.22	0.50	14.51
448	03 44 47.61	32 17 14.4	1.70	19.12	0.82	1.23	0.46	14.79
466	03 44 30.40	32 14 58.2	1.54	18.45	0.80	1.05	0.34	14.78
469	03 44 49.47	32 12 18.1	1.63	18.92	0.70	1.20	0.47	14.84
485	03 44 32.38	32 08 03.2	1.73	18.92	0.82	1.08	0.37	14.63
502	03 44 38.84	32 14 47.7	1.86	19.14	0.89	1.12	0.45	14.67
509	03 45 06.97	32 14 03.9	1.36	18.37	...	0.98	0.37	15.12
546	03 44 27.83	32 08 00.4	1.41	20.41	0.83	0.93	0.50	16.00
574	03 44 52.36	32 11 27.4	1.27	19.60	0.71	0.75	0.45	16.14
581	03 44 41.24	32 12 16.4	...	21.93	0.20	1.61	0.70	16.39
584	03 44 43.82	32 11 54.1	...	...	...	2.20	0.92	15.90
588	03 44 24.57	32 11 40.6	...	20.64	0.95	1.42	0.57	15.56
594	03 44 38.58	32 11 04.8	...	21.90	1.23	1.70	0.61	16.08
745	03 44 24.29	32 06 11.8	...	20.48	0.97	1.40	0.39	15.77
901	03 44 50.47	32 12 09.5	1.30	20.47	0.68	1.07	0.60	16.25
917	03 44 48.36	32 12 26.4	...	20.72	1.04	1.34	0.58	15.66
943	03 44 16.36	32 12 53.9	1.23	18.72	0.47	0.72	0.28	16.09
951	03 44 10.86	32 13 00.6	1.15	18.13	0.52	0.86	0.17	15.44
959	03 44 09.80	32 13 07.1	1.44	19.75	0.60	0.85	0.49	16.34
998	03 44 53.49	32 13 56.9	1.60	20.07	0.75	1.00	0.38	16.25
1007	03 45 02.81	32 14 07.6	2.47	19.80	0.92	1.10	0.58	15.38
1020	03 44 36.31	32 14 19.9	...	20.87	1.05	1.54	0.72	14.98
1021	03 44 59.07	32 14 22.8	1.47	18.67	0.72	0.95	0.37	15.02
1062	03 44 48.14	32 15 22.4	...	19.47	0.80	1.14	0.44	14.87
1110	03 45 00.78	32 16 35.7	1.71	20.14	0.74	1.08	0.41	16.07
1139	03 44 59.68	32 17 30.3	1.84	19.01	0.78	1.23	0.42	14.58
1142	03 44 55.39	32 17 34.9	1.65	19.28	0.75	1.04	0.37	15.53
1167	03 44 32.68	32 18 06.1	1.30	19.99	...	1.16	0.51	15.99
1173	03 44 53.81	32 18 12.1	1.60	19.23	0.70	0.87	0.34	15.87
1194	03 45 02.04	32 18 36.3	2.10	18.36	0.86	1.25	0.46	13.93
1555	03 44 23.09	32 15 12.2	...	19.86	0.73	1.27	0.29	16.21
1729	03 44 25.41	32 13 56.5	1.38	19.05	0.69	0.83	0.34	15.76
1735	03 44 08.33	32 13 57.4	1.18	19.54	0.59	0.64	0.01	17.13
1742	03 44 21.65	32 13 47.8	1.31	17.65	0.59	0.85	0.26	14.75
3076	03 44 56.39	32 13 35.8	...	21.32	0.98	0.79	0.82	16.66
3104	03 45 01.75	32 14 34.4	...	20.04	0.78	0.69	0.62	15.00
3117	03 44 49.41	32 15 04.8	...	22.16	1.04	1.62	0.73	16.21
3215	03 44 46.55	32 13 50.5	...	22.04	1.03	1.52	0.61	16.36
4053	03 44 14.89	32 06 12.2	...	21.58	1.07	1.36	0.77	15.70
22253	03 44 23.73	32 17 16.2	...	18.28	0.57	0.02	0.09	15.55

<sup>a</sup>From the 2MASS Point Source Catalog for 509, from Luhman (1999) for 584 and 1167, and from Luhman et al. (2003) for the remaining objects.

<sup>b</sup>From Herbig (1998) for 222 and 546 and from Luhman (1999) for the remaining objects.

<sup>c</sup>From Luhman (1999) for 411, 509, and 1167 from Luhman et al. (2003) for the remaining objects.

<sup>d</sup>Luhman et al. (2003).

<sup>e</sup>Muench et al. (2003).

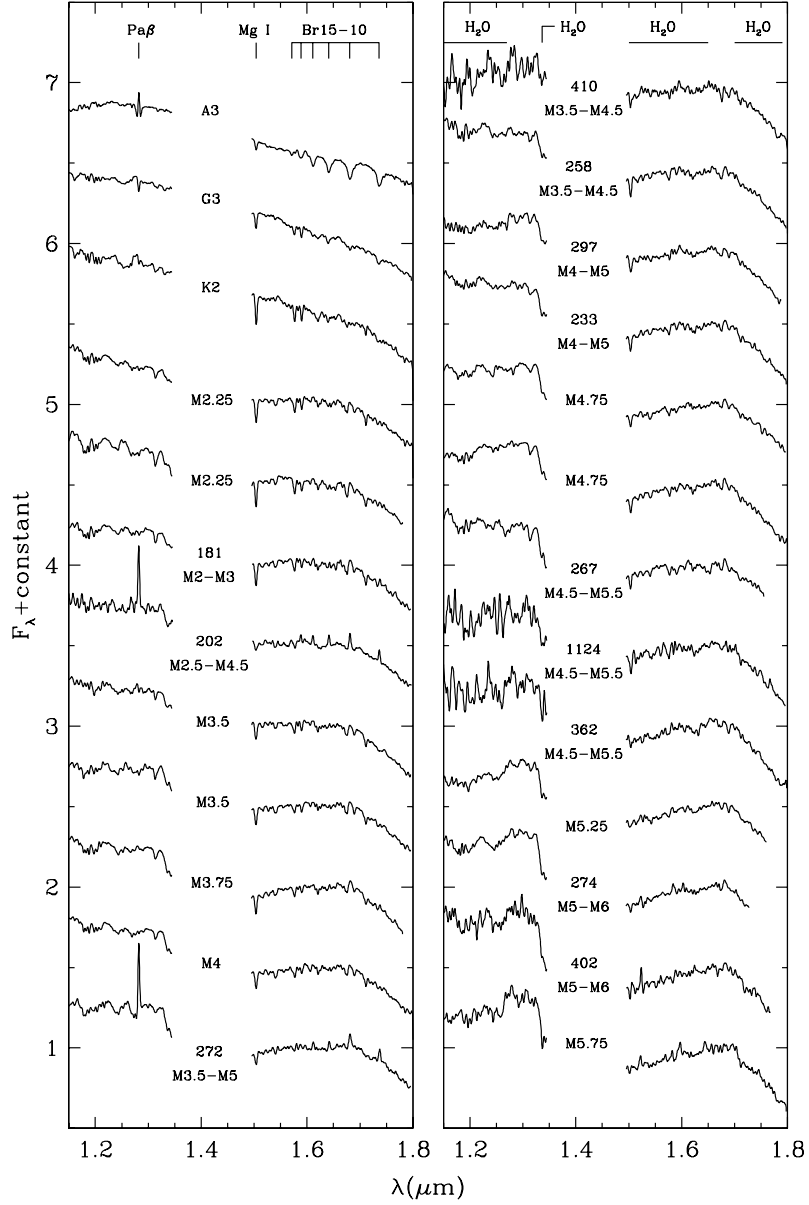


Fig. 1.— FLAMINGOS near-IR spectra of objects toward the IC 348 cluster with spectral types earlier than M6. Previously known members are labeled with only their optical classifications. New members are labeled with their identifications and the spectral types derived from a comparison to the IR spectra of the optically-classified members. The spectra are displayed at a resolution of  $R = 500$ , normalized at  $1.68 \mu\text{m}$ , and dereddened (§ 3.1).

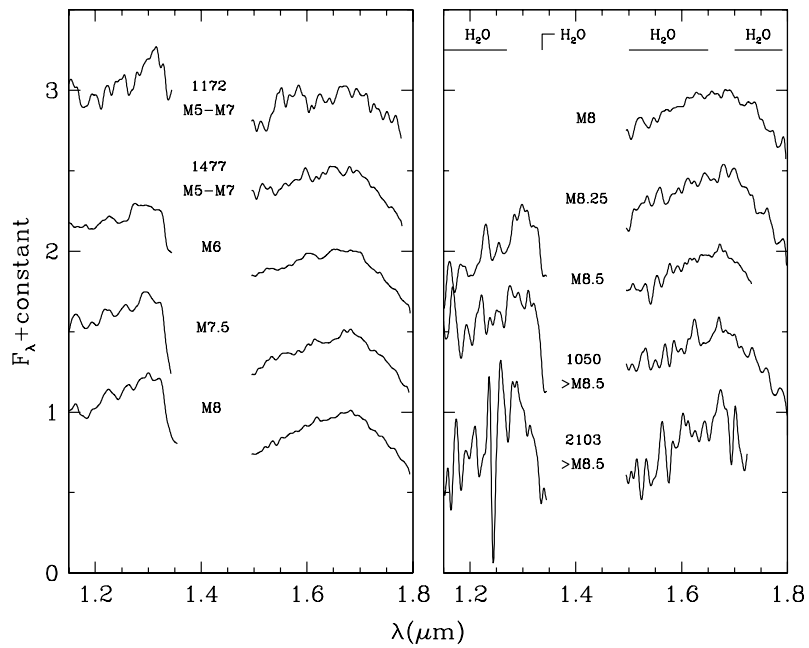


Fig. 2.— FLAMINGOS near-IR spectra of objects toward the IC 348 cluster with spectral types of M6 and later. Previously known members are labeled with only their optical classifications. New members (1172, 1477) and candidate members (1050, 2103) are labeled with their identifications and the spectral types derived from a comparison to the IR spectra of the optically-classified members. The spectra are displayed at a resolution of  $R = 200$ , normalized at  $1.68 \mu\text{m}$ , and dereddened (§ 3.1).

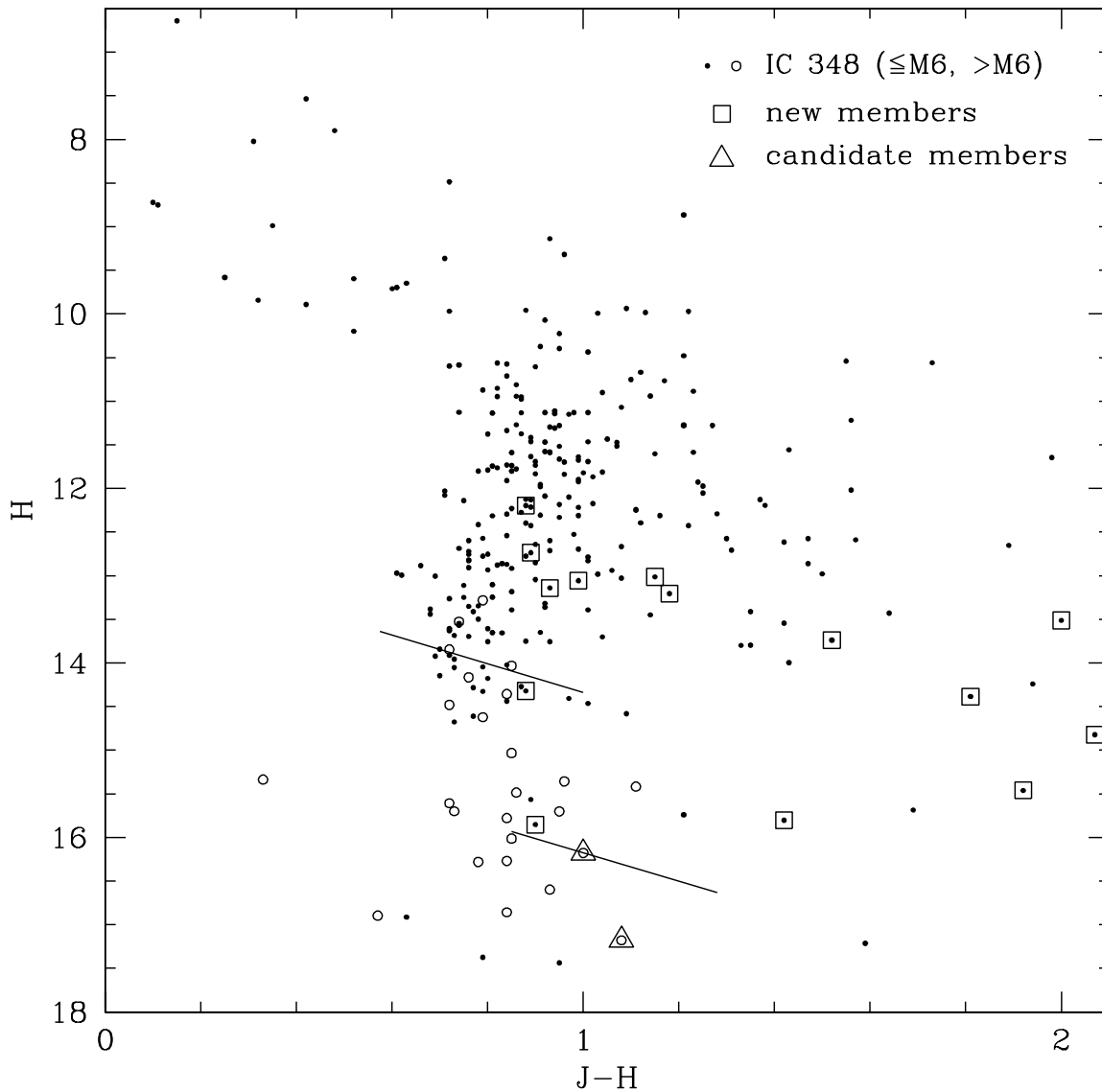


Fig. 3.—  $J - H$  versus  $H$  for all known members of the IC 348 cluster at  $\leq M6$  and  $> M6$  (*points and circles*) that have been identified through spectroscopy in this work (*boxes*) and in previous studies. We also include two late-type objects from our spectroscopic sample that lack definitive classifications of membership (*triangles*). The reddening vectors from  $A_V = 0-4$  are plotted for  $0.08$  ( $\sim M6.5$ ) and  $0.02 M_\odot$  ( $\sim M9$ ) for ages of 3 Myr (*upper and lower solid lines*) (Chabrier et al. 2000). Most of these  $J$  and  $H$  measurements are from 2MASS and Muench et al. (2003).

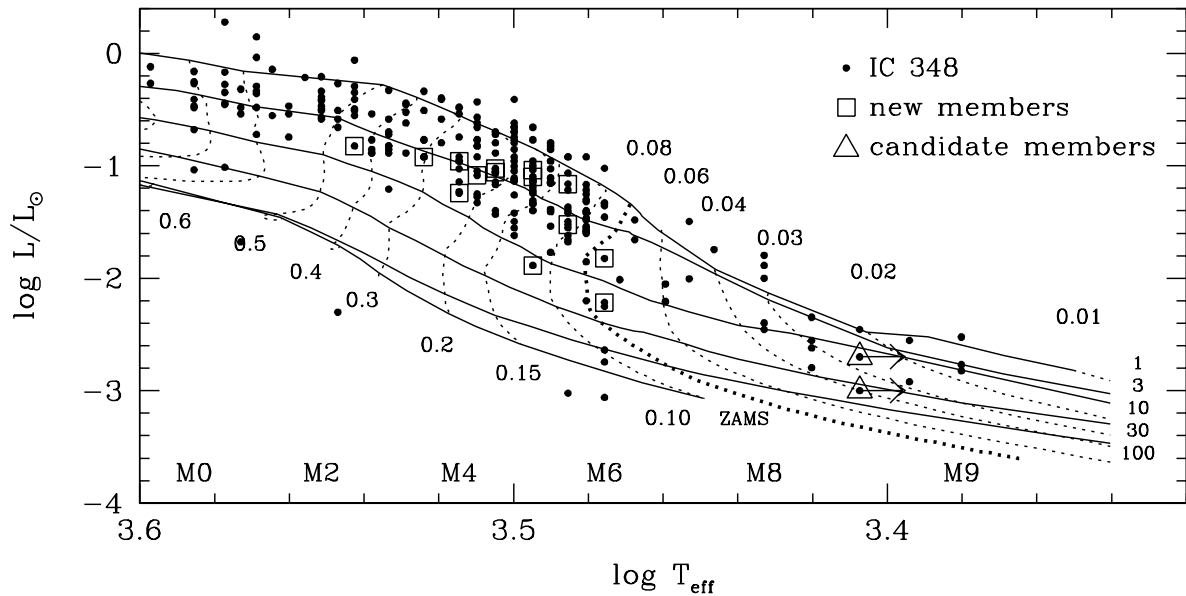


Fig. 4.— H-R diagram for the IC 348 cluster with the same symbols as in Figure 3, except that both early and late-type members are shown as points. We include the theoretical evolutionary models of Baraffe et al. (1998) ( $M/M_{\odot} > 0.1$ ) and Chabrier et al. (2000) ( $M/M_{\odot} \leq 0.1$ ), where the mass tracks (*dotted lines*) and isochrones (*solid lines*) are labeled in units of  $M_{\odot}$  and Myr, respectively. The data for the previously known members are from Luhman et al. (2003).